Multi-UAV Cooperative Moving Target Search Based on Improved Pigeon-Inspired Optimization

Weiming Zheng[1], Delin Luo[1], Zhenwen Zhou[1], Yang Xu[2,3], and Yan Chen[4](✉)

[1] School of Aerospace Engineering, Xiamen University, Xiamen 361102, China
[2] School of Civil Aviation, Northwestern Polytechnical University, Xi'an 710072, China
[3] Yangtze River Delta Research Institute of NPU, Taicang 215400, China
[4] The Fifth Electronics Research Institute of the Ministry of Industry and Information Technology, Guangzhou 511370, China
chenyan1@ceprei.com

Abstract. Aiming at the problem of multi-UAV cooperative moving target search, a cooperative search decision based on improved pigeon-inspired optimization is designed. Firstly, based on the independence of moving targets, a target probability information graph model with normal distribution is established. In order to improve the certainty of the presence of the target in the environment, the information graph of the certainty of the search environment is established. Secondly, the attractant and repulsive digital pheromone graphs are established to guide the UAV to fly to the unsearched area, reducing the probability of repeated search and improving the efficiency of collaborative target search. Based on the traditional pigeon-inspired optimization, it is improved by adding speed update and correction mechanism and elite generation mechanism. Then, combining with the existence probability information of the target in the environment and the detection information of the UAV searching for the target, the improved pigeon-inspired optimization is used to determine the optimal searching flight path of the UAV. Finally, the feasibility and effectiveness of the improved pigeon-inspired optimization for the collaborative search of moving targets are verified by setting different search flight step sizes and using different search algorithms in simulation experiments.

Keywords: Multi-UAV · Cooperative search · Moving target · Digital pheromones · Improved pigeon-inspired optimization

1 Introduction

Using UAVs to search and make a reconnaissance of the battlefield environment is the most extensive application of UAVs in the military field [1], and it is also a hot topic in the field of UAV research [2]. In the actual battlefield environment, it is necessary not only to detect stationary targets distributed in the mission area, but also to search for

Z. Ren et al. (Eds.): *Proceedings of 2021 5th Chinese Conference on Swarm Intelligence and Cooperative Control*, LNEE 934, pp. 921–930, 2023.
https://doi.org/10.1007/978-981-19-3998-3_88

moving targets in the environment. With the search flight of multi-UAV, the probability of moving targets appearing in the searched area increases, so it is necessary to design the corresponding algorithm to improve the return search of the searched area by UAVs and improve the efficiency of searching for moving targets.

Qi [3] added digital pheromone model to reduce the probability of searching the same area between *UAVs, which improved* the search efficiency of moving targets. Zhen [4] combined the artificial potential field method with ant colony algorithm and proposed a task planning scheme for intelligent coordination of multiple UAVs. *Duan* [5] proposed an optimization algorithm inspired by pigeons' orientation recognition ability. Up to now, pigeon-inspired optimization has made a lot of scientific research achievements in trajectory planning [6] and other fields due to its advantages of two-stage iterative solution and simple algorithm model.

The remaining of the paper is organized as follows. Section 2 gives the establishments of the search environment model and UAV flight dynamic model. Section 3 gives the target probability distribution information graph and search environment digital information graph. Section 4 designs a moving target cooperative search decision based on improved pigeon-inspired optimization. Section 5 is the simulation comparison experiment. Section 6 concludes the paper.

2 Problem Description

In this paper, the search area is rasterized into multiple identical regular quadrilateral cells. The irregular obstacle area and threat area in the environment are filled into quadrilateral regular area. It is assumed that the UAV flies at a constant speed during the whole search mission, moves one environmental unit in one unit of time, and stays at the center of the environmental unit in each flight.

It is assumed that the UAVs perform search tasks in the same flight plane, and the two-dimensional dynamic model of the UAV is considered, ignoring the dimension of altitude h. The two-dimensional UAV dynamic model is shown as follow:

$$\begin{cases} \dot{x} = v\cos\varphi \\ \dot{y} = v\sin\varphi \\ \dot{\varphi} = \omega \end{cases} \tag{1}$$

where x, y represent the horizontal and vertical coordinates of the UAV, v denotes the velocity of the UAV, φ denotes the heading Angle of the UAV in the horizontal plane and ω denotes the angular velocity of the UAV.

Considering that the change of UAV's heading Angle φ is constrained by the factor of minimum turning radius, the UAV's maximum heading angle is set to 45°.

The targets existence probability values $P_{mn}^{x,y} \in [0, 1]$ are set for each environment unit environment (x, y). $P_{mn}^{x,y} = 0$ indicates that the targets must not exist in the unit environment (x, y) and is generally used to mark the flight obstacle area. $P_{mn}^{x,y} = 1$ indicates the target must exist in the cell environment (x, y).

According to the actual flight environment of UAVs, the search environment can be divided into common search areas, key search areas and flight obstacle areas by setting different target probability values.

Let event $E_{mn}^{x,y} = 1$ indicate the presence of a target in environment (x, y) and $D_{mn}^{x,y}(t) = 1$ indicates that the sensors detect the presence of the target at time t. Thus,

$$\begin{cases} p_d = P(D_{mn}^{x,y}(t) = 1 | E_{mn}^{x,y} = 1) \\ 1 - p_d = P(D_{mn}^{x,y}(t) = 0 | E_{mn}^{x,y} = 1) \\ p_f = P(D_{mn}^{x,y}(t) = 1 | E_{mn}^{x,y} = 0) \\ 1 - p_f = P(D_{mn}^{x,y}(t) = 0 | E_{mn}^{x,y} = 0) \end{cases} \tag{2}$$

where $p_f \in (0, 1)$ denotes the false alarm rate of detection targets and $p_d \in (0, 1)$ denotes the detection rate of the sensors. Based on the Bayesian criterion, when the UAV detects the target in environment (x, y) at time $t + 1$, namely $D_{mn}^{x,y}(t + 1) = 1$,the target existence probability of the environment unit is updated as:

$$P_{mn}^{x,y}(t+1) = P(E_{mn}^{x,y} = 1 | D_{mn}^{x,y}(t+1) = 1) = \frac{p_d P_{mn}^{x,y}(t)}{p_f(1 - P_{mn}^{x,y}(t)) + p_d P_{mn}^{x,y}(t)}. \tag{3}$$

In the same way, when $D_{mn}^{x,y}(t + 1) = 0$, we can obtain:

$$P_{mn}^{x,y}(t+1) = P(E_{mn}^{x,y} = 1 | D_{mn}^{x,y}(t+1) = 0) = \frac{(1 - p_d) P_{mn}^{x,y}(t)}{(1 - p_f)(1 - P_{mn}^{x,y}(t)) + (1 - p_d) P_{mn}^{x,y}(t)}. \tag{4}$$

Based on the probability of the presence of a target in the environment, the UAV detection sensor determines whether there is a target or not:

$$\begin{cases} 1, P_{mn}^{x,y}(t) > \xi_p, \\ 0, P_{mn}^{x,y}(t) \le \xi_p. \end{cases} \tag{5}$$

3 Moving Target Information Graph

3.1 Probability Distribution Information Graph

As the UAVs enter the search areas to carry out the search task, the targets will move randomly around with the initial position as the center, and their position information is independent increment. According to [7], wiener stochastic process can be used to describe the random movement characteristics of time-sensitive targets:

$$P_{mn}^{x,y}(t) = \sum_{i=1}^{N_t} \frac{1}{2\pi(\sigma_0^2 + \sigma_e^2 t)} e^{-\frac{(x - x_t^i)^2 + (y - y_t^i)^2}{2(\sigma_0^2 + \sigma_e^2 t)}} \tag{6}$$

where σ_e is a constant indicating the variance of wiener stochastic process, σ_0 is a constant indicating the variance of the Gaussian distribution.

3.2 Environment Determination Graph

In order to reduce the uncertainty of the targets in the search environment as soon as possible and guide the UAVs to search in the direction with a large gradient of uncertainty reduction, the uncertainty information graph is used to describe the certainty information of the UAVs in the search environment.

$$X_{mn}^{x,y}(t) = \begin{cases} \eta X_{mn}^{x,y}(t-1), & (x,y) \text{ hasn't been detected,} \\ X_{mn}^{x,y}(t-1) + \eta(1 - X_{mn}^{x,y}(t-1)), & (x,y) \text{ has been detected.} \end{cases} \tag{7}$$

where η is the attenuation factor of the information certainty in the environment. With the detection of the raster environment (x, y) by UAVs, the certainty of the existence of the target will increase.

In order to improve the return rates of UAVs to the detected area that has not been re-explored for a long time, the time threshold is set to appropriately reduce the certainty of the searched area and guide UAVs to conduct search flight to the area again.

$$X_{mn}^{x,y}(t) = \eta X_{mn}^{x,y}(t-1), \Delta t > \delta_T. \tag{8}$$

Δt is the time interval between two detections of the grid cell $(x, y).\delta_T$ is the time threshold.

3.3 Digital Pheromone Graph

Inspired by the behavior characteristics of colony organisms, digital pheromone mechanism is introduced into cooperative flight decision of multi-UAV. Based on the search map, the whole search areas are endowed with certain pheromone content.

The attractor digital pheromone is defined as S_a. It is updated as follows:

$$S_a^{x,y}(t) = (1 - E_a)[(1 - G_a)(S_a^{x,y}(t-1) + K_s^{x,y}(t) \cdot D_a) + g_a^{x,y}(t)] \tag{9}$$

where $S_a^{x,y}(t)$ denotes the attractor pheromone content in the grid environment (x, y) at the time of t, $E_a \in (0, 1)$ denotes the volatilization coefficient of attractor pheromone, $G_a \in (0, 1)$ denotes the propagation coefficient of attractor pheromone to surrounding grid cells, and K_s is a $\{0, 1\}$ matrix.

When the two search intervals of the same grid unit reach the threshold, the release switch of the attractor pheromone of the unit will be turned on, the digital pheromone content of the unit will be increased, and the UAV will be guided to the unit for return detection.

In (9), D_a denotes the self-released content of attractor pheromone, $g_a^{x,y}(t)$ denotes the pheromone content of the attractor pheromone propagated from the surrounding grid cell to the (x, y) during time $t - 1$ to t. The influence range of pheromone propagation is defined as 8 neighboring cells in a circle around the grid of the cell. The calculation formula of attractant pheromone propagation is as follows:

$$g_a^{x,y}(t) = \frac{1}{N_s} \sum_{i=1}^{N_s} G_a(S_{a,i}^{x,y}(t-1) + K_{s,i}^{x,y}(t) \cdot D_a), \tag{10}$$

where N_s represents the total number of surrounding transmission grids.

Similarly, let the repulsion pheromone S_r update as follows:

$$S_r^{x,y}(t) = (1 - E_r)\{(1 - G_r)[S_r^{x,y}(t-1) + (1 - K_s^{x,y}(t)) \cdot D_r] + g_r^{x,y}(t)\}, \quad (11)$$

The calculation formula of repulsion pheromone propagation is as follows:

$$g_r^{x,y}(t) = \frac{1}{N_s}\sum_{i=1}^{N_s} G_r[S_{r,i}^{x,y}(t-1) + (1 - K_{s,i}^{x,y}(t)) \cdot D_r]. \quad (12)$$

4 Decision-Making of Multi-UAV Cooperative Search

4.1 Cooperative Search Objective Function

At time t, the total reward function J_t of UAVs searching moving target mainly consists of three parts: target search reward J_p, environmental search reward J_e and collaborative search reward J_s:

$$J_{\mathrm{t}} = \sum_{i=1}^{L_f} (\omega_p J_p(i) + \omega_e J_e(i) + \omega_s J_s(i)), \quad (13)$$

where $\omega_p + \omega_e + \omega_s = 1$. Each UAV has a detection radius of $R_f.L_f$ is the length of the UAV's flight path.

$$J_p(i) = \sum_{j=1}^{N_{i,R}} (p_d - p_f)P_{mn}^{x_i,y_i}(j) + p_f, \quad (14)$$

$$J_e(i) = \sum_{j=1}^{N_{i,R}} X_{mn}^{x_i,y_i}(j) - X_{mn}^{x_{i-1},y_{i-1}}(j-1), \quad (15)$$

$$J_s(i) = \sum_{j=1}^{N_{i,R}} S_a^{x_i,y_i}(j) - S_r^{x_i,y_i}(j). \quad (16)$$

4.2 Improved Pigeon-Inspired Optimization

Assume that the initial size of the pigeon swarm is N_p. The ith pigeon's initial two-dimensional position information X_p^i and its velocity V_p^i. They update as:

$$\begin{cases} X_p^i = V_p^i(t-1)e^{-R_p t} + rand() \cdot (X_{p,g} - X_p^i(t-1)), \\ V_p^i = X_p^i(t-1) + V_p^i(t)). \end{cases} \quad (17)$$

where t is current iteration times, $R_p \in (0, 1)$ is the map and compass, $rand()$ is a random number between (0, 1) and $X_{p,g}$ is the optimal position in the pigeon swarm in the last iteration period.

The swarm follow the central pigeon to update their flight positions while weeding out the disoriented pigeons:

$$N_p(t) = \frac{N_p(t-1)}{2}, \tag{18}$$

$$X_{p,c}(t) = \frac{\sum_{i=1}^{N_p(t)} X_p^i(t-1) \cdot Fit(X_p^i(t-1))}{N_p(t) \sum_{i=1}^{N_p(t)} Fit(X_p^i(t-1))} \tag{19}$$

$$X_p^i(t) = X_p^i(t-1) + rand() \cdot (X_{p,c}^i(t) - X_p^i(t-1)). \tag{20}$$

(18) denotes the number of lost pigeons eliminated in each iteration period. $Fit(x)$ is the fitness value of the problem that each pigeon represents. $X_{p,c}(t)$ is the position information of the central pigeon in the iteration period t.

In the iteration of map and compass operator in the first stage of pigeon-inspired optimization, the flight velocities values of pigeon swarms are too discrete in the process of updating, that is, the difference between the maximum value and the minimum value may be too large, resulting in the convergence speed of the algorithm in the iterative solution is too slow.

By improving the design, the updated velocities values are limited between $V_{\max}$ and $V_{\min}$. In (22), after the pigeon velocity updates, a size determination mechanism is added:

$$V_p^i(t) = \begin{cases} V_{min}, & V_p^i(t) < V_{\min}, \\ V_{max}, & V_p^i(t) > V_{\max}, \\ V_p^i(t), & \text{else}. \end{cases} \tag{21}$$

In order to accelerate the convergence speed of pigeon-inspired optimization in iterative solution, the optimal $N_{p,e} = w_p N_p$ pigeons in the population are taken as the elite generation, $w_p \in [0.2, 0.5]$. Then the elite generation is added into the new swarm for population recombination, so that the current optimal solution existed in each generation and the convergence speed of optimal solution is accelerated. The process of improved pigeon-inspired optimization is shown in Table 1.

In order to avoid collision, the artificial potential field method is used to make each UAV generate a certain repulsive force. The closer the distance between the UAVs is, the greater the repulsive force will be, so that the UAVs will search and fly in the direction away from each other.

For the ith UAV, the joint force produced by other UAVs is:

$$\boldsymbol{F}_i(t) = \sum_{j=1, j\neq i}^{N_u} \boldsymbol{F}_{ij}(t), \tag{22}$$

Table 1. Improved pigeon-inspired optimization.

Steps of improved pigeon-inspired optimization
Initialize X_p, V_p, T_{p1}, T_{p2} ;
for $t = 2,3,...,T_{p1}$ **do**
for $i = 1,2,...,N_p$ **do**
Calculate and update V_p^i ;
Fixed the velocity value by V_{max}, V_{min} ;
Calculate and update X_p^i ;
Calculate the fitness values $Fit(X_p^i)$ of each pigeon;
end for
Rank $Fit(X_p^i)$ from highest to lowest and the first $N_{p,e}$ pigeons are taken out as elite generation;
Take the elite generation from the previous generation and regroup them, keeping the swarm size at N_p ;
end for
for $t = 2,3,...,T_{p2}$ **do**
Calculate the fitness values $Fit(X_p^i)$ and rank them from highest to lowest;
Weed out stray pigeons and calculate N_p ;
for $i = 1,2,...,N_p$ **do**
Add up the fitness value of the pigeon;
end for
Calculate the position $X_{p,c}$ of the central pigeon in the swarm;
for $i = 1,2,...,N_p$ **do**
Calculate the position X_p^i of the uneliminated pigeons by $X_{p,c}$
end for
end for
Outputs the information of pigeons with the best fitness in the swarm;

$$\boldsymbol{F}_{ij} = \begin{cases} k_f e^{-\omega_f D_{ij} \boldsymbol{E}_{ji}}, \ D_{ij} \leq D_{\max}, \left|\phi_{ij}\right| \leq \phi_{\max}, \\ 0, \ \text{others}. \end{cases} \tag{23}$$

For UAV$_i$, $\boldsymbol{F}_i(t)$ is the cumulative force vector generated by other UAV$_j$.$\boldsymbol{F}_{ij}(t)$ is the repulsive force vector generated between UAV$_i$ and UAV$_j$.k_f and ω_f are constants. D_{ij} is the vertical shortest distance between UAVs in the flight heading direction.E_{ji} is the unit vector in the direction of the force generated by UAV$_j$ to UAV$_i$, and the force increases with the smaller distance between UAVs.

4.3 Decision-Making Steps

The decision-making steps of multi-UAV cooperative search for moving targets are as follows:

1. Calculate the targets' distribution information graph in Sect. 3.1.
2. Initialize the environment determination graph in Sect. 3.2.
3. According to Sect. 3.3, establish the attraction and repulsion pheromone graph of the search environment.
4. Initialize the search location and flight direction of each UAV. Regard the flight path's increment value of the UAV as the pigeon in the swarm. Initialize the population size of the pigeon swarm.
5. According to the objective function in Sect. 4.1, calculate the target search reward, environmental search reward and cooperative search reward.
6. According to the Table 1 in Sect. 4.2, the optimal search flight path is solved through the iterative optimization of compass operator and landmark operator.
7. Using the collision avoidance model in Sect. 4.2, the flight path avoiding collision is selected as the next search flight path for UAV's final decision.
8. Judge whether the multi-UAV search task is over. If not, go to step4.

5 Simulation

Figure 1 shows the comparison simulation of traditional and improved pigeon-inspired optimization. The aim is to find the minimum of the objective function and the objective function of the simulation experiment is $f(x, y) = x^2 - 10\cos(2\pi y) + 10$,where $x, y \in [-5.12, 5.12]$. $PIO_{1\sim4}$ in Fig. 1 represent the pigeon-inspired optimization whether added with the speed constraints and elite generation. PIO_1 is added with nothing while PIO_4 representing the method presented in this paper is added with both.

The results show that the improved pigeon-inspired optimization designed in this paper has smaller discreteness and faster convergence rate in solving the problem, and the optimization effect is more obvious than the traditional way.

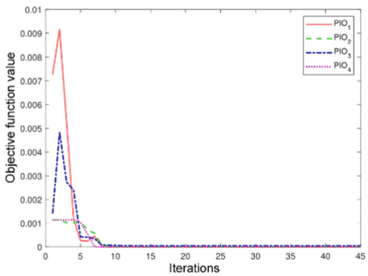

Fig. 1. Optimization efficiency of IPIO

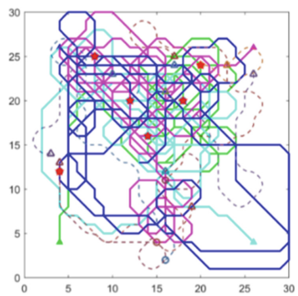

Fig. 2. Cooperative search trajectories of IPIO

Rasterize the search area into 30×30 units and each unit denotes 1km^2. Set $N_t = 4$. Therefore, 4 UAVs are used to enter the four corners of the search area. In the search area, 10 moving targets randomly appears, which means $N_u = 10$. Set $X_{mn}(t_0) = 1$, $p_d = 0.8$, $p_f = 0.2$, $G_a = 0.3$, $E_a = 0.4$, $D_a = 1$, $G_r = 0.3$, $E_r = 0.4$ and $D_r = 1$. Each UAV flies at a velocity of 200 m/s. The velocities of the moving targets are random in [20 m/s,100 m/s]. The period of simulation experiment is 5 s.

Figure 2 is the simulation result of improved pigeon-inspired optimization search with UAV's flight step k = 300. The solid triangles are marked as the initial search flight positions of the UAVs, and the solid lines are their search path. The hollow triangles are marked as the initial positions of the randomly distributed targets, the circles are marked as their terminal position, and the dotted lines are the motion tracks.

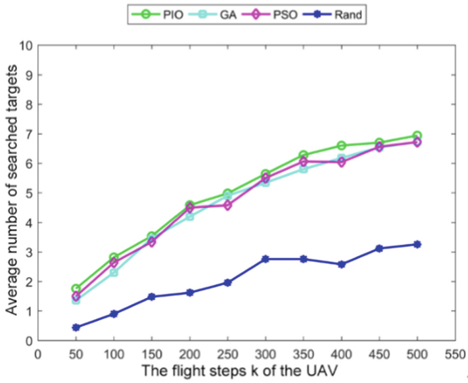

Fig. 3. Average number of searched targets by 4 different methods

In order to better analyze and compare the search efficiency of different methods applied to moving target search, 50 simulation experiments are carried out for different flight search steps K, and the average value of the results are obtained in Fig. 3. PIO denotes the improved pigeon-inspired optimization in this paper. GA denotes genetic algorithm. PSO denotes particle swarm optimization algorithm. Rand denotes random search algorithm. Compared with 3 different algorithms, the improved pigeon-inspired optimization searches more targets and has higher search efficiency.

6 Conclusion

In this paper, a cooperative search method based on improved pigeon-inspired optimization is presented. By establishing and updating the attraction and repulsion pheromone graph, UAVs can be guided to the unsearched area, and the repeated search probability can be reduced to improve UAVs search flight efficiency. In order to search the target moving to the searched area, a time threshold mechanism is set to improve the return search rate of UAVs. Simulation verified the effectiveness of the presented method.

Acknowledgment. This work was supported by Science and Technology on Avionics Integration Laboratory and Aeronautical Science Foundation of China under Grant No. 20185568005. The corresponding author of this work is Chen Yan.

References

1. Duan, H., Shen, Y., Zhao, Y., et al.: Review of technological hotspots of unmanned aerial vehicle in 2020. Sci. Technol. Rev. **39**(1), 233–247 (2021)
2. Xu X., Duan, H., Zeng, Z., et al.: Progresses in UAV/USV cooperative control. In: Aero Weaponry, vol. 27, no. 6, pp. 1–6 (2020)
3. Qi, X., Wei, R., Shen, D., et al.: Distributed cooperative search methods of multi-UAV based on prediction of moving targets. Syst. Eng. Electron. **36**, 2417–2425 (2014)
4. Zhen, Z., Chen, Y., Wen, L., et al.: An intelligent cooperative mission planning scheme of UAV swarm in uncertain dynamic environment. Aerosp. Sci. Technol. 105826 (2020)
5. Duan, H., Qiu, H., Fan, Y., et al.: Unmanned aerial vehicle close formation cooperative control based on predatory escaping pigeon-inspired optimization. Sci. Sin. Technol. **45**(6), 559–572 (2015)
6. Huo Mengzhen F., Duan Haibin, S., Yang Qing, T., E.T.: Live-fly experimentation for pigeon-inspired obstacle avoidance of quadrotor unmanned aerial vehicles, Science China Information Sciences 62 (5), 52201 (2019)
7. Vinh K: Optimal Cooperative Tasking and Coordination of UAVs in a Search and Coverage Mission, North Carolina Agricultural and Technical State University (2019)